

Performance benchmarks of an array-based hand-held photoacoustic probe adapted from a clinical ultrasound system for non-invasive sentinel lymph node imaging

Chulhong Kim, Todd N. Erpelding, Ladislav Jankovic and Lihong V. Wang

Phil. Trans. R. Soc. A 2011 **369**, 4644-4650
doi: 10.1098/rsta.2010.0353

References

This article cites 15 articles, 3 of which can be accessed free

<http://rsta.royalsocietypublishing.org/content/369/1955/4644.full.html#ref-list-1>

Email alerting service

Receive free email alerts when new articles cite this article - sign up in the box at the top right-hand corner of the article or click [here](#)

To subscribe to *Phil. Trans. R. Soc. A* go to:
<http://rsta.royalsocietypublishing.org/subscriptions>

Performance benchmarks of an array-based hand-held photoacoustic probe adapted from a clinical ultrasound system for non-invasive sentinel lymph node imaging

BY CHULHONG KIM^{1,†}, TODD N. ERPELDING², LADISLAV JANKOVIC²
AND LIHONG V. WANG^{1,*}

¹*Optical Imaging Laboratory, Department of Biomedical Engineering, Washington University in St Louis, Campus Box 1097, One Brookings Drive, St Louis, MO 63130-4899, USA*

²*Philips Research North America, 345 Scarborough Road, Briarcliff Manor, NY 10510, USA*

Clinical translation of photoacoustic (PA) imaging can be facilitated by integration with commercial ultrasound (US) scanners to enable dual-modality imaging. An array-based US scanner was modified for hand-held PA imaging. The performance was benchmarked in terms of signal-to-noise ratio (SNR), axial spatial resolution and sensitivity. PA images of a tube, filled with methylene blue (MB; approx. 30 mM) and placed at various depths in chicken tissue, were acquired. A 5 cm penetration depth was achieved with an 18.6 dB SNR using a laser fluence of 3 mJ cm^{-2} , only one-seventh of the safety limit (20 mJ cm^{-2}). An axial resolution of approximately $400 \mu\text{m}$ was maintained at all imaging depths. The PA sensitivity to MB placed 2.3 cm deep in chicken tissue was less than $100 \mu\text{M}$. Further, after intradermal injection of MB (approx. 30 mM), a rat sentinel lymph node was clearly identified *in vivo*, beneath a 3.8 cm thick layer of chicken breast. The accumulated concentration of MB in the node was estimated to be approximately 7 mM. The noise-equivalent sensitivities (approx. 2 cm depth) were 17 and $85 \mu\text{M}$, *ex vivo* and *in vivo*, respectively. These results support the use of this PA system for non-invasive mapping and image-guided needle biopsy of sentinel nodes in breast cancer patients.

Keywords: photoacoustic imaging; clinical ultrasound array system; sentinel lymph node biopsy; image-guided needle biopsy

1. Introduction

Photoacoustic (PA) imaging represents an emerging, non-invasive, non-ionizing hybrid modality combining both optical excitation and ultrasonic detection. It can provide high resolution, deep penetration and high optical absorption

*Author for correspondence (chulhong@buffalo.edu).

†Present address: Department of Biomedical Engineering, University at Buffalo, State University of New York, 328 Bonner Hall, Buffalo, NY 14260, USA.

One contribution of 20 to a Theo Murphy Meeting Issue ‘Illuminating the future of biomedical optics’.

sensitivity [1]. Owing to its unique ultrasonic detection, PA imaging can overcome the fundamental issues of pure optical imaging, such as shallow penetration depth or poor spatial resolution [2,3]. Using either intrinsic (e.g. haemoglobin and melanin) or extrinsic (e.g. organic dyes and nanoparticles) contrast, high-resolution PA imaging can provide highly sensitive morphological, functional and molecular information about biological tissues [4–6]. Further, conventional ultrasonic scanners can serve as PA wave receivers, thus combining the high contrast of optical imaging and the high resolution of ultrasound (US) imaging [7–10].

We have previously reported *in vivo* PA and US mapping of rat sentinel lymph nodes (SLNs) using a hand-held probe adapted from a clinical US imaging system [10–12]. Clinically used dyes, including methylene blue (MB) and indocyanine green, have been successfully tested with this hand-held probe. In the work reported in this paper, we quantified signal-to-noise ratio (SNR), axial spatial resolution and sensitivity of the hand-held PA probe by measuring both chicken tissues *ex vivo* and rats *in vivo*.

2. Method and materials

The combined PA and US imaging system was developed around a commercial clinical US scanner (iU22, Philips Healthcare) and has been described previously [10–12]. In brief, a tunable dye laser (PrecisionScan-P, Sirah), pumped by a Q-switched Nd : YAG laser (PRO-350-10, Newport), produced 6.5 ns laser pulses at a repetition rate of 10 Hz, which illuminated tissue via bifurcated fibre bundles (CB18043, Fiberguide). An optical wavelength of 650 nm, close to the peak optical absorption wavelength of MB (667 nm), was used. Light fluence on the surface was approximately 3 mJ cm^{-2} , only one-seventh of the ANSI [13] safety limit (20 mJ cm^{-2}). Generated PA waves were detected by a linear array US probe (L8-4, Philips Healthcare) with a nominal bandwidth of 4–8 MHz. PA images were reconstructed using a Fourier beam-forming algorithm [14] and displayed at approximately 1 frame per second.

A plastic tube (7 mm in diameter \times 25 mm in length) filled with MB was embedded in chicken breast tissues. The diameter of the tube is comparable in size with human axillary lymph nodes. By layering additional chicken breast tissue, we increased the imaging depth, as measured by US imaging. In addition, the PA sensitivity for detecting MB was measured by varying the concentration of MB within the tube placed at a depth of approximately 2.3 cm in chicken breast tissue from 0.1 to 30 mM. *Ex vivo* chicken breast experiments were used to quantify the SNR, noise-equivalent sensitivity and axial spatial resolution. The SNR was defined as the mean of PA signals obtained from the tube filled with MB divided by the standard deviation of the background PA signals. The noise-equivalent sensitivity was defined as the ratio between MB dye concentration and SNR. The axial spatial resolution at various imaging depths in chicken breast tissue was measured as the full width at half maximum of the one-dimensional profile taken across the tube boundary.

Animal care and use were in accordance with approved guidelines at Washington University in St Louis. We imaged Sprague Dawley rats (approx. 200 g) under anaesthesia after injection of a mixture of ketamine (80 mg kg^{-1}) and

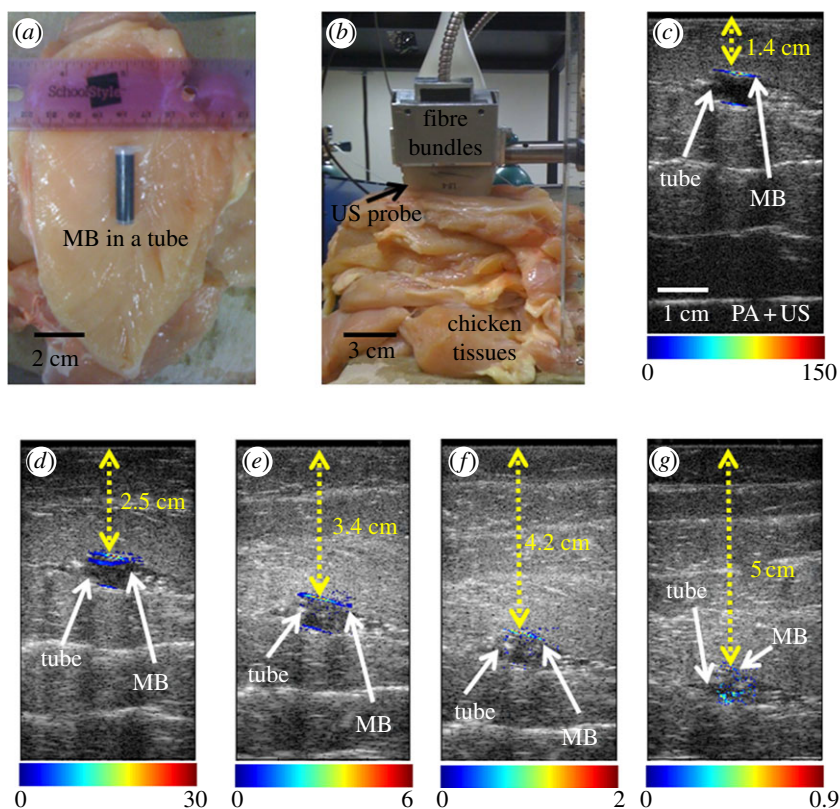


Figure 1. Photoacoustic (PA) imaging of methylene blue (MB) in biological tissues. Photographs of (a) the tube filled with MB as positioned (b) within a stack of chicken breast tissue. Overlaid PA (pseudocolour) and US (greyscale) images of the tube containing MB at depths of (c) 1.4 cm, (d) 2.5 cm, (e) 3.4 cm, (f) 4.2 cm and (g) 5 cm. Pseudocolour represents the optical absorption in laboratory units. (Online version in colour.)

xylazine (8 mg kg^{-1}). For *in vivo* imaging, we placed chicken breast tissue atop the rats to increase the imaging depth. Clear US coupling gel was applied between layers of chicken breast and the rat skin surface to maintain effective acoustic coupling. A control PA image was acquired before intradermal injection of MB into the left forepaw. After injection of MB (0.1 ml, 30 mM), a series of PA images were acquired to identify SLNs enhanced by MB. Further, MB accumulation was visually confirmed in SLNs during post-mortem dissection.

3. Results and discussion

The SNR and axial spatial resolution of the PA imaging system were quantified by embedding a plastic tube filled with MB dye at various depths within chicken breast tissue (figure 1a). As shown in figure 1b, the imaging depth was incremented by stacking approximately 1 cm thick chicken breast slices. Note that for all imaging depths measured, the tube was surrounded by approximately 5 cm

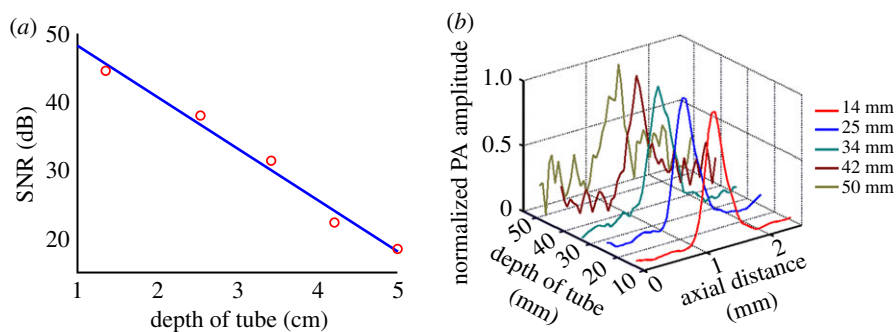


Figure 2. Plots of (a) signal-to-noise ratio (SNR) in decibels and (b) axial resolution as a function of depth of the tube containing approximately 30 mM of methylene blue. (Online version in colour.)

of chicken breast tissue on each side and the bottom. To improve the SNR, PA signals were averaged 80 times. Figure 1*c–g* shows overlaid PA and US images of the blue dye-containing tube embedded at various depths within the surrounding chicken tissues. All US images are displayed in greyscale with the same dynamic range, whereas all PA images are in pseudocolour with different dynamic ranges. The pseudocolour in each PA image represents optical absorption, defined as the product of local optical fluence and the optical absorption coefficient of the blue dye-filled tube, in laboratory units. Structural US images helped us to confirm the origins of received PA signals.

Figure 2*a* is a plot of the SNR as a function of the depth of the tube. The SNR in decibels decreased linearly with increasing depth. The measured penetration depth for 1/e decay in chicken breast tissue is approximately 1.16 cm, which matches well with the value reported in the literature (approx. 1.13 cm) at an optical wavelength of 650 nm [15]. The 5 cm penetration depth (approx. 4.3 times the 1/e optical penetration depth) was achieved with an SNR of 18.6 dB, corresponding to an 18.7 dB attenuation from the skin surface. The 1/e penetration depth in human breast is 0.78 cm at 656 nm [16]. Note that the 5 cm penetration depth, the distance between the top surface of the chicken breast tissue (measured by US imaging) and the top surface of the MB-containing tube (measured by PA imaging), was achieved with a laser fluence of 3 mJ cm^{-2} (only one-seventh of the ANSI safety limit). Using a laser fluence of 20 mJ cm^{-2} (the ANSI safety limit), the penetration depth can theoretically be increased to approximately 7.4 cm. The axial resolutions measured from the tube boundaries at all imaging depths in chicken breast tissue were approximately 400 μm (figure 2*b*), which was close to the theoretical axial resolution (approx. 385 μm, for a nominal bandwidth of 4–8 MHz).

To investigate the PA sensitivity for detecting MB, we imaged a tube positioned approximately 2.3 cm deep within the chicken breast tissue. The mean depth of the top surface of human SLNs is 1.2 ± 0.5 cm. Thus, our imaging depth was greater than the depths of most SLNs encountered clinically. The concentration of MB varied from 0.1 to 30 mM (figure 3*a*). As shown in figure 3*b*, the SNR increased with increasing concentrations approximately linearly. PA signals were detected at a concentration of 100 μM (13×10^{-12} mol with $0.4 \times 0.4 \times 1 \text{ mm}^3$ voxel size) with an SNR of 15.7 dB. Therefore, the

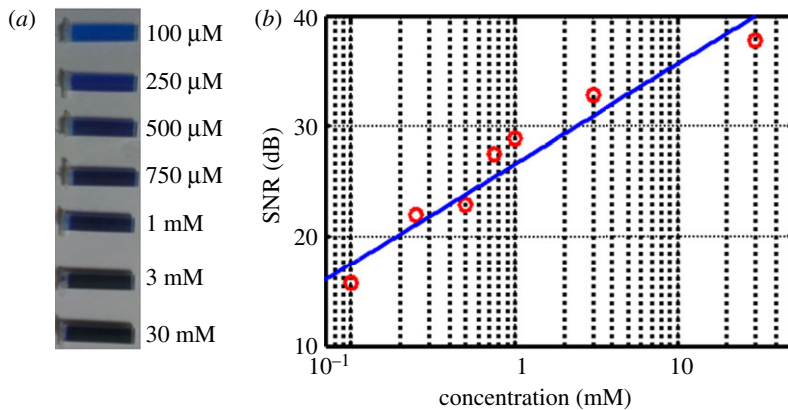


Figure 3. (a) Photograph showing the tubes filled with varying concentrations of methylene blue (MB). (b) Plot of photoacoustic signal-to-noise ratio (SNR) as a function of MB concentration at a depth of 2.3 cm. (Online version in colour.)

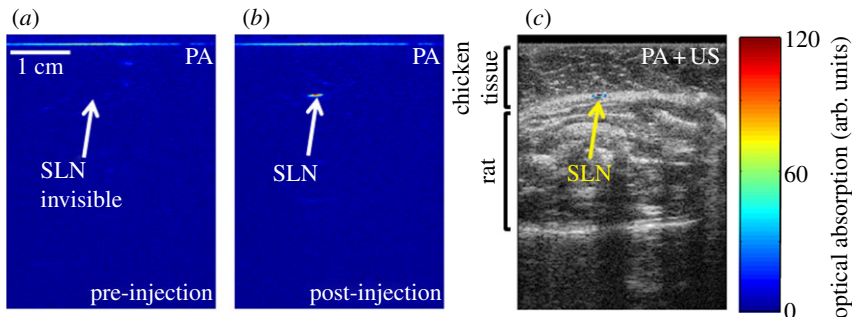


Figure 4. *In vivo* photoacoustic (PA) mapping of rat sentinel lymph nodes (SLNs). (a) Control PA image acquired before methylene blue (MB) injection. (b) PA image taken after MB injection. (c) Overlaid post-injection PA (pseudocolour) and US (greyscale) images. Pseudocolour represents the optical absorption in laboratory units. (Online version in colour.)

noise-equivalent sensitivity is $17\ \mu\text{M}$ at a depth of 2.3 cm in chicken breast tissues. Figure 4 shows *in vivo* PA and US mapping of rat SLNs with MB. We imaged the left axillary region in a rat before (figure 4a) and after (figure 4b) MB injection. Soon after injection (within 5 min), MB flowed through lymphatic vessels near the injection site in the left forepaw and accumulated in the SLN (approx. 1 cm deep), which was identified photoacoustically. The structural US image (grey colour) and functional PA image (pseudocolour, MB uptake in the SLN) are overlaid in figure 4c. Moreover, we overlaid additional chicken breast tissue atop the targets to increase the imaging depth. The SLN containing MB was clearly seen at all measured depths, as shown in Figure 5a–d, achieving an *in vivo* 3.8 cm SLN imaging depth with an SNR of 21 dB. This penetration depth was approximately 50 per cent greater than the previously reported depth (2.5 cm) [11]. The SNR (dB) was plotted as a function of the imaging depth (figure 5e). The measured *in vivo* penetration depth for $1/e$ decay is 1.06 cm, which matches well with the above-mentioned *ex vivo* $1/e$ penetration depth (1.16 cm). Further, we estimated

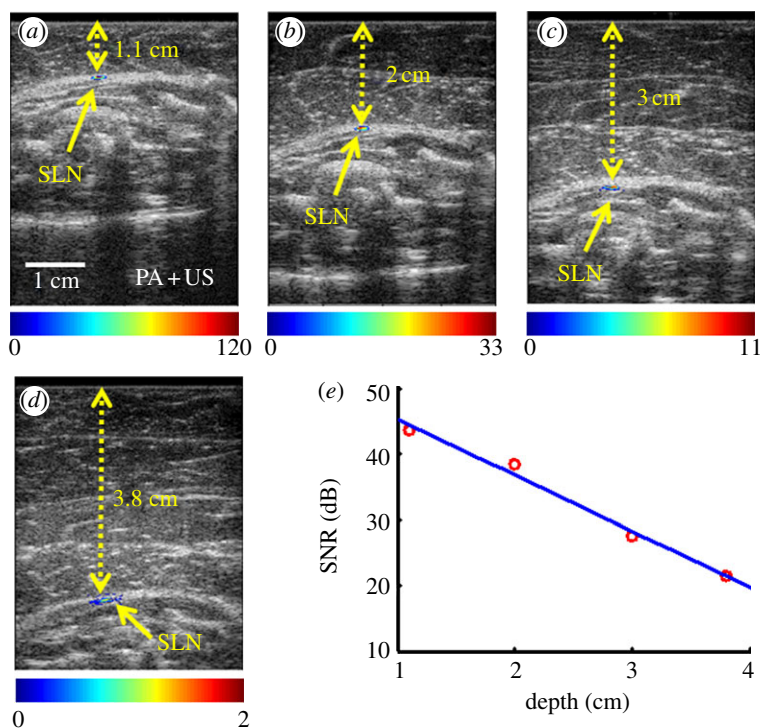


Figure 5. *In vivo* photoacoustic (PA) mapping of rat sentinel lymph nodes (SLNs) and ultrasound (US) mapping of surrounding anatomical structure. The depth of the SLN from the imaging surface was varied to (a) 1.1 cm, (b) 2 cm, (c) 3 cm and (d) 3.8 cm by overlaying chicken tissue atop the rat. Pseudocolour represents the optical absorption in laboratory units. (e) Plot of PA SNR as a function of depth of the SLN. (Online version in colour.)

the actual concentration of MB in the SLN using curve fitting in figure 3 to be approximately 7 mM ($0.3 \mu\text{mol}$ with $3 \times 3 \times 3 \text{ mm}^3$ lymph node size). Therefore, the *in vivo* noise-equivalent sensitivities were 85 and $592 \mu\text{M}$ at depths of 2 and 3.8 cm, respectively.

4. Conclusions

The capabilities—including SNR, axial resolution and sensitivity—of the hand-held PA imaging probe were quantified in biological tissues. The maximum penetration depth reached approximately 5 cm, and the sensitivity was better than $100 \mu\text{M}$ at a depth of 2.3 cm.

The noise-equivalent sensitivities were 17 and $85 \mu\text{M}$ *ex vivo* (2.3 cm deep) and *in vivo* (2 cm deep), respectively. The axial resolution was maintained over the imaging depths observed. Further, the estimated optical property (effective attenuation coefficient) of chicken breast tissue matched well with previously reported values. Moreover, *in vivo* PA and US mapping of rat SLNs at an imaging depth of approximately 3.8 cm was successfully accomplished following MB injection.

This work was supported in part by grants from the National Institutes of Health (R01 EB000712, R01 EB008085, R01 CA134539, U54 CA136398, R01 EB010049 and 5P60 DK02057933). L.V.W. has a financial interest in Microphotoacoustics, Inc. and in Endra, Inc., which, however, did not support this work.

References

- 1 Wang, L. V. 2009 Multiscale photoacoustic microscopy and computed tomography. *Nat. Photon.* **3**, 503–509. (doi:10.1038/nphoton.2009.157)
- 2 Zeff, B. W., White, B. R., Dehghani, H., Schlaggar, B. L. & Culver, J. P. 2007 Retinotopic mapping of adult human visual cortex with high-density diffuse optical tomography. *Proc. Natl Acad. Sci. USA* **104**, 12 169–12 174. (doi:10.1073/pnas.0611266104)
- 3 Jung, W., McCormick, D. T., Zhang, J., Wang, L., Tien, N. C. & Chen, Z. 2006 Three-dimensional endoscopic optical coherence tomography by use of a two-axis microelectromechanical scanning mirror. *Appl. Phys. Lett.* **88**, 163901. (doi:10.1063/1.2195092)
- 4 Kim, C., Favazza, C. & Wang, L. V. 2010 *In vivo* photoacoustic tomography of chemicals: high-resolution functional and molecular optical imaging at new depths. *Chem. Rev.* **110**, 2756–2782. (doi:10.1021/cr900266s)
- 5 Kim, C. *et al.* 2010 *In vivo* molecular photoacoustic tomography of melanomas targeted by bioconjugated gold nanocages. *ACS Nano* **4**, 4559–4564. (doi:10.1021/nn100736c)
- 6 Kim, C., Song, K. W., Gao, F. & Wang, L. V. 2010 Sentinel lymph nodes and lymphatic vessels: noninvasive dual-modality *in vivo* mapping by using indocyanine green in rats: volumetric spectroscopic photoacoustic imaging and planar fluorescence imaging. *Radiology* **255**, 442–450. (doi:10.1148/radiol.10090281)
- 7 Niederhauser, J. J., Jaeger, M., Lemor, R., Weber, P. & Frenz, M. 2005 Combined ultrasound and optoacoustic system for real-time high-contrast vascular imaging *in vivo*. *IEEE Trans. Med. Imaging* **24**, 436–440. (doi:10.1109/TMI.2004.843199)
- 8 Emelianov, S., Li, P.-C. & O'Donnell, M. 2009 Photoacoustics for molecular imaging and therapy. *Phys. Today* **62**, 34–39. (doi:10.1063/1.3141939)
- 9 Fronheiser, M. P., Ermilov, S. A., Brecht, H. P., Conjusteau, A., Su, R., Mehta, K. & Oraevsky, A. A. 2010 Real-time optoacoustic monitoring and three-dimensional mapping of a human arm vasculature. *J. Biomed. Opt.* **15**, 021305. (doi:10.1117/1.3370336)
- 10 Kim, C. *et al.* 2010 Hand-held array-based photoacoustic probe for guiding needle biopsy of sentinel lymph nodes. *J. Biomed. Opt.* **15**, 046010. (doi:10.1117/1.3469829)
- 11 Erpelding, T. N., Kim, C., Pramanik, M., Jankovic, L., Maslov, K., Guo, Z., Margenthaler, J. A., Pashley, M. D. & Wang, L. V. 2010 Noninvasive photoacoustic and ultrasonic imaging of rat sentinel lymph nodes with a clinical ultrasound system. *Radiology* **256**, 102–110. (doi:10.1148/radiol.10091772)
- 12 Kim, C., Erpelding, T. N., Jankovic, L., Pashley, M. D. & Wang, L. V. 2010 Deeply penetrating *in vivo* photoacoustic imaging using a clinical ultrasound array system. *Biomed. Opt. Express* **1**, 278–284. (doi:10.1364/BOE.1.000278)
- 13 ANSI. 2002 American national standard for the safe use of lasers. Standard Z136.1–2000, ANSI Inc., New York, USA.
- 14 Kostli, K. P., Frenz, M., Bebie, H. & Weber, H. P. 2001 Temporal backward projection of optoacoustic pressure transients using Fourier transform methods. *Phys. Med. Biol.* **46**, 1863–1872. (doi:10.1088/0031-9155/46/7/309)
- 15 Marquez, G., Wang, L. V., Lin, S. P., Schwartz, J. A. & Thomsen, S. L. 1998 Anisotropy in the absorption and scattering spectra of chicken breast tissue. *Appl. Opt.* **37**, 798–804. (doi:10.1364/AO.37.000798)
- 16 Spinelli, L., Torricelli, A., Pifferi, A., Taroni, P., Danesini, G. M. & Cubeddu, R. 2004 Bulk optical properties and tissue components in the female breast from multiwavelength time-resolved optical mammography. *J. Biomed. Opt.* **9**, 1137–1142. (doi:10.1117/1.1803546)